

HSRI VERSION OF THE IMPROVED THREE
DIMENSIONAL COMPUTER SIMULATION OF VEHICLE
CRASH VICTIMS. VOLUME I. ANALYSIS.

Prepared by:

R. O. Bennett
D. H. Robbins
Highway Safety Research Institute
Institute of Science and Technology
University of Michigan
Ann Arbor, Michigan 48109

FINAL REPORT. CONTRACT DOT-HS-7-01659

Prepared for:

U. S. Department of Transportation
National Highway Traffic Safety Administration
Washington, D.C. 20590

Date:

March 8, 1982

UMTRI The University of Michigan
Transportation Research Institute

On September 16 1982, the Regents of
The University of Michigan changed the
name of the Highway Safety Research
Institute to the University of Michigan
Transportation Research Institute (UMTRI)

Technical Report Documentation Page

1. Report No.		2. Government Accession No.		3. Recipient's Catalog No.	
4. Title and Subtitle HSRI Version of the Improved Three Dimensional Computer Simulation of Vehicle Crash Victims. Volume 1. Analysis.				5. Report Date March 8, 1982	
				6. Performing Organization Code	
7. Author(s) R. O. Bennett and D. H. Robbins				8. Performing Organization Report No. UM-HSRI-82-8-1	
9. Performing Organization Name and Address Highway Safety Research Institute Institute of Science and Technology The University of Michigan Ann Arbor, Michigan 48109				10. Work Unit No. 015935	
				11. Contract or Grant No. DOT-HS-7-01659	
12. Sponsoring Agency Name and Address U. S. Department of Transportation National Highway Traffic Safety Administration Washington, D.C. 20590				13. Type of Report and Period Covered Final October 1977 - March 1982	
				14. Sponsoring Agency Code	
15. Supplementary Notes					
16. Abstract <p>The purpose of this project has been to expand the Crash Victim Simulation software, originally developed at Calspan Corp. The objectives were to:</p> <ol style="list-style-type: none"> 1. review the capability of advanced features of the software; 2. improve the contact algorithm in the CVS; 3. develop software for use in correlation and validation studies; and, 4. apply the software to problems in side impact. <p>This report is organized in three volumes which are supplementary to existing CVS documentation. The first volume describes the analysis of new features (moveable contact surfaces, sharing of deflections between ellipsoids and contact surfaces, and bivariate representation of force-deflection characteristics in deflection as well as deflection rate). This volume is intended for the analyst who wishes to understand the basic assumptions incorporated in this model. Volume II presents an updated User's Manual for the entire CVS model which is expected to serve as sufficient documentation for the ordinary user of the model. Volume III presents information concerning the CVS model as a computer program and is intended for professional programmers who need to study or make changes in the program.</p>					
17. Key Words Crash Victim Simulation Crash Dynamics Occupant Dynamics Side Impact Dynamics				18. Distribution Statement Unlimited	
19. Security Classif. (of this report) Unclassified		20. Security Classif. (of this page) Unclassified		21. No. of Pages 44	22. Price

NOTICE

This document is disseminated under the sponsorship of the Department of Transportation in the interest of information exchange. The United States Government assumes no liability for the contents or use thereof.

TABLE OF CONTENTS

	<u>Page</u>	
1.0 INTRODUCTION	1	—
1.1 General	1	—
1.2 Organization of Report	1	—
1.3 Scope of Changes	1	—
1.4 References	2	—
2.0 ELLIPSOID-PLANE CONTACT DETERMINATION	4	—
2.1 Definition of Penetration	4	—
2.2 Calculation of Maximum Penetration for the Mid-Panel Case	8	—
2.3 Penetration of Edge One	11	—
2.4 Penetration at a General Edge	12	—
2.5 Penetrations at Edges Two, Three, and Four	14	—
2.6 Calculation of Edge Effects	19	—
2.7 Tangential Forces	21	—
2.8 Recognition of Being Behind the Panel	24	—
2.9 Calculation of Solid Corner Effects	24	—
3.0 LOAD-DEFLECTION PROPERTIES	28	—
3.1 Loading Characteristics	28	—
3.2 Unloading Characteristics	28	—
3.3 Reloading Characteristics	32	—
3.4 Bivariate Table Interpolation	32	—
3.5 Saturation and Breakdown	33	—
4.0 SHARED DEFLECTION	36	—
4.1 General Algorithm	38	—
4.2 First Order Bivariate Polynomial Case	40	—
4.3 Sixth Order Univariate Polynomial Case	41	—
4.4 General Pure Deflection Case	42	—
4.5 Tabular Case	43	—

TABLE OF FIGURES

	<u>Page</u>
1. Ellipsoid Seen in Panel System	5
2a. X-Z Intersection Ellipse	6
2b. Y-Z Projection Ellipse	6
3. Minimum Above Panel Boundary	7
4. Minimum Below Panel Boundary	7
5. Panel Nomenclature	8
6. The Edge System	12
7. Discontinuity of Edges	19
8. Edge Sealing Factor Zones	20
9. The Solid Corner Situation	24
10. Panel Treated as Part of Solid Corner	26
11. Mutual Deformation of an Ellipsoid on a Panel	37

1.0 INTRODUCTION

1.1 General

The purpose of this project has been to expand the Crash Victim Simulation software, originally developed at Calspan Corp. The objectives were to: 1. review the capability of advanced features of the software; 2. improve the contact algorithm in the CVS; 3. develop software for use in correlation and validation studies; and, 4. apply the software to problems in side impact. This three volume report considers the first two of the objectives.

1.2 Organization of Report

This report is organized in three volumes. The first volume deals with the analysis of the new features and is supplementary to the initial CVS writeups (1) and updates (2). This volume is intended for the analyst who wishes to understand the basic assumptions incorporated in this model. The second volume presents an updated user's manual for the entire CVS model as now constituted and is expected to serve as sufficient documentation for the ordinary user of the model. The third volume presents information concerning the CVS model as a computer program and is intended for professional programmers who need to make changes in the program.

Volume One contains sections dealing with the new ellipsoid-plane contact algorithms, the material properties now available, and shared deflection.

Volume Two contains sections dealing with the updated, machine-produced input writeup, a general description of output options and an example run.

Volume Three contains sections describing the layout of packing tables for variable information, the structure of the program and a detailed layout of possible output from the program.

1.3 Scope of Changes

The HSRI Version of the CALSPAN CVS Model is based on Version 18A of that model augmented by some of the corrections of Version 19 con-

cerning Euler joints. HSRI refined the contact algorithms for ellipsoid-panel interactions. Three important basic problems in the contact algorithms were addressed. The first problem is accurate computation of deflections even for the case of complete penetration of an ellipsoid into a contact surface. The second problem is the computation of contact forces based on mutual deformation of the interacting elements. The third problem is handling of permanent deformation by contact surfaces.

The contact section of the old CVS was largely replaced with an algorithm based on the approach taken in earlier HSRI models(3,4,5) incorporating some of the ideas of British Leyland (6). In our early dealings with the old CVS, we modified the input section to read and check the ID field of the input cards. In addition, we modified the output section to use only one logical device and to print optionally in equal increments of simulated time. These changes were made to partially facilitate the use of the model. A more general specification of vehicle initial conditions and more flexibility in reporting of kinematics were later incorporated for the same reason. In general, we have followed the policy of making changes only where such changes were defensible by their utility to Occupant Side Impact Simulation.

1.4 References

1. Fleck J. T., Butler, F. E., Vogel, S. L., "An Improved Three-Dimensional Computer Simulation of Vehicle Crash Victims", Calspan Corp., Buffalo, 4 vols., NTIS Nos. PB241692-5.
2. Butler, F. E., Addendices to reference 1., A-K, Calspan Corp., Buffalo, unpublished.
3. Robbins, D. H., Bennett, R. O., and Roberts, V. L., "HSRI Three-Dimensional Crash Victim Simulation: Analysis, Verifications; Users' Manual, and Pictorial Section," HSRI, The University of Michigan, Ann Arbor, NTIS No. PB208242, June, 1971.
4. Robbins, D. H., Bennett, R. O., and Bowman, B. M., "HSRI Six-Mass, Three-Dimensional Crash Victim Simulation," HSRI, The University of Michigan, Ann Arbor, NTIS No. PB239476, Feb. 1973, 302 p.
5. Bowman, B. M., Bennett, R. O., and Robbins, D. H., "MVMA Two-Dimensional Crash Victim Simulation, Version 3," HSRI, The University of Michigan, Ann Arbor, 3 vols., NTIS Nos. PB235753/1, 236907/2, 236908/0, 684 p., 1974.

6. Butterfield, K. R., "The Computation of the Maximum Penetration of an Ellipsoid Through a Panel," Report No. NA2, British Leyland, unpublished, July 1976, 5 p.

2.0 Ellipsoid-Plane Contact Determination

A body segment in the form of an ellipsoid contact and penetrates a vehicle panel in the form of a parallelogram. To determine the force that is developed by this contact, a penetration depth, δ , must first be determined. This section presents expressions for penetration due to the various possible ellipsoid-panel contacts.

Section 2.1 describes the geometry and defines penetration for mid-plane, edge, and corner contacts.

Section 2.2 presents a derivation of expressions for the mid-panel case.

Section 2.3 deals with penetration at edge one.

Section 2.4 deals with penetration at a general edge.

Section 2.5 presents the results of Section 2.4 for each of the other three edges.

2.1 Definition of Penetration

We define an x, y, z , coordinate system by taking the x - y plane as the panel surface with the positive x -axis along one edge. The coordinates of the center of the ellipsoid in this system are (x_0, y_0, z_0) . The principle axes of the ellipsoid are ξ, η, ζ with semi-major axes lengths of a, b, c respectively so that the ellipsoid equation in this system is: (Refer to Figure 1.)

$$\frac{\xi^2}{a^2} + \frac{\eta^2}{b^2} + \frac{\zeta^2}{c^2} = 1 \quad (1)$$

The two systems are related by

$$\begin{pmatrix} x \\ y \\ z \end{pmatrix} = D \begin{pmatrix} \xi \\ \eta \\ \zeta \end{pmatrix} + \begin{pmatrix} x_0 \\ y_0 \\ z_0 \end{pmatrix} \quad (2)$$

where

$$D = \begin{pmatrix} d_{11} & d_{12} & d_{13} \\ d_{21} & d_{22} & d_{23} \\ d_{31} & d_{32} & d_{33} \end{pmatrix} = \begin{pmatrix} \hat{k} \cdot \hat{e}_1 & \hat{k} \cdot \hat{e}_2 & \hat{k} \cdot \hat{e}_3 \\ \hat{j} \cdot \hat{e}_1 & \hat{j} \cdot \hat{e}_2 & \hat{j} \cdot \hat{e}_3 \\ \hat{i} \cdot \hat{e}_1 & \hat{i} \cdot \hat{e}_2 & \hat{i} \cdot \hat{e}_3 \end{pmatrix}$$

and where $\hat{i}, \hat{j}, \hat{k}$ are unit vectors in the x, y, z system and $\hat{e}_1, \hat{e}_2, \hat{e}_3$ are unit vectors in the ξ, η, ζ system.

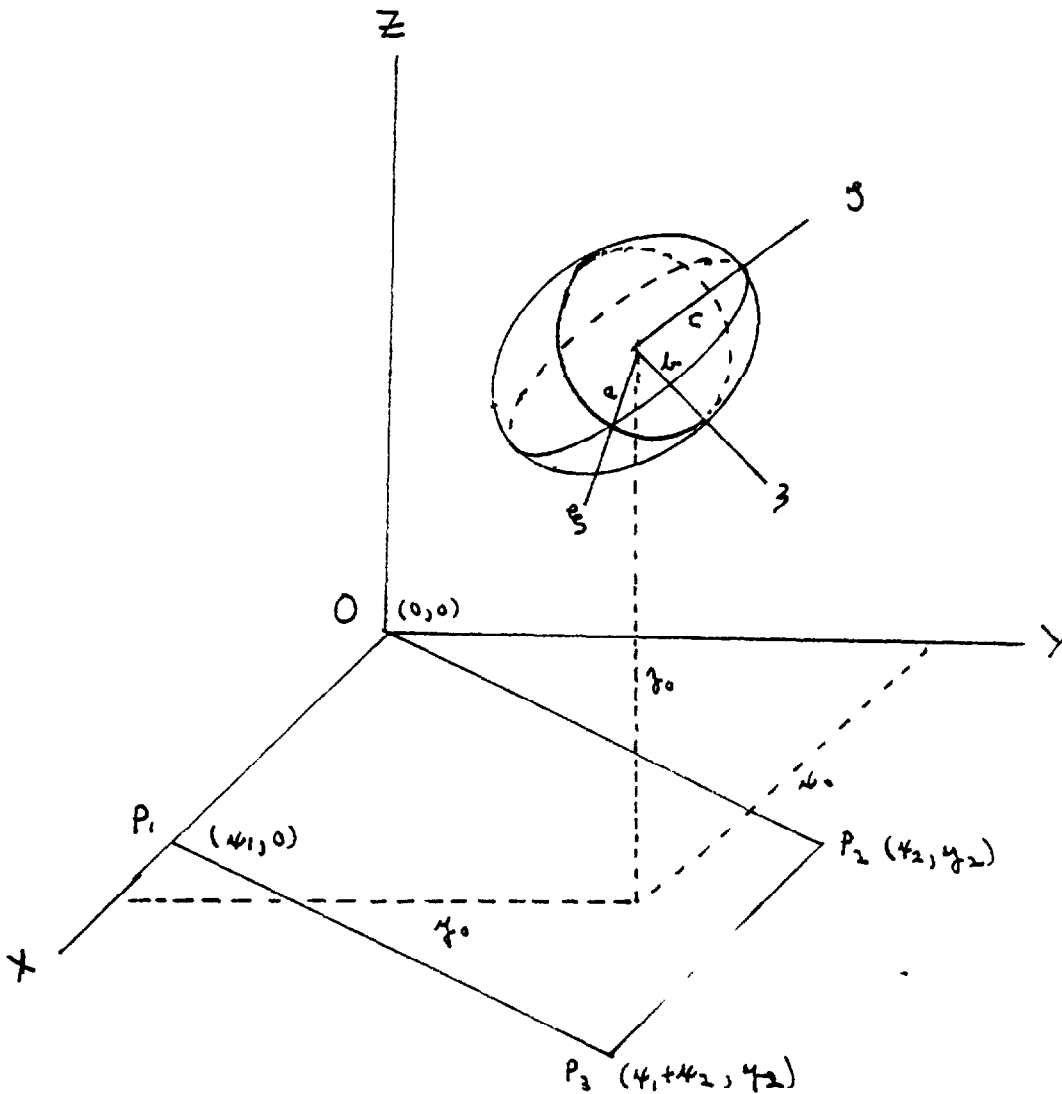


Figure 1 Ellipsoid Seen In Panel System

The z value of the point on the ellipsoid which attains the absolute minimum z value (the lowest point of the ellipsoid) will be termed $-\delta$ max. If this point lies within the panel boundary and is beneath its surface, then we define penetration δ to be equal to δ max.

Even if the location of δ_{\max} is outside the panel boundary, there is still a possibility of intersection with one or more of the edges of the panel. In this case, we determine a lowest point for each of the four edges of the panel define each edge penetration to be the negative of the z coordinate of the corresponding low point, and finally define penetration to be maximum of the four: $\delta = \max \{ \delta_1, \delta_2, \delta_3, \delta_4 \}$.

An edge penetration can best be described for the edge formed by line segment OP_1 in figure 1 (edge one); the other edges are entirely similar. Figure 2 illustrates two views of edge one. Figure 2a shows the x - z plane in the panel system while figure 2b shows the y - z plane.

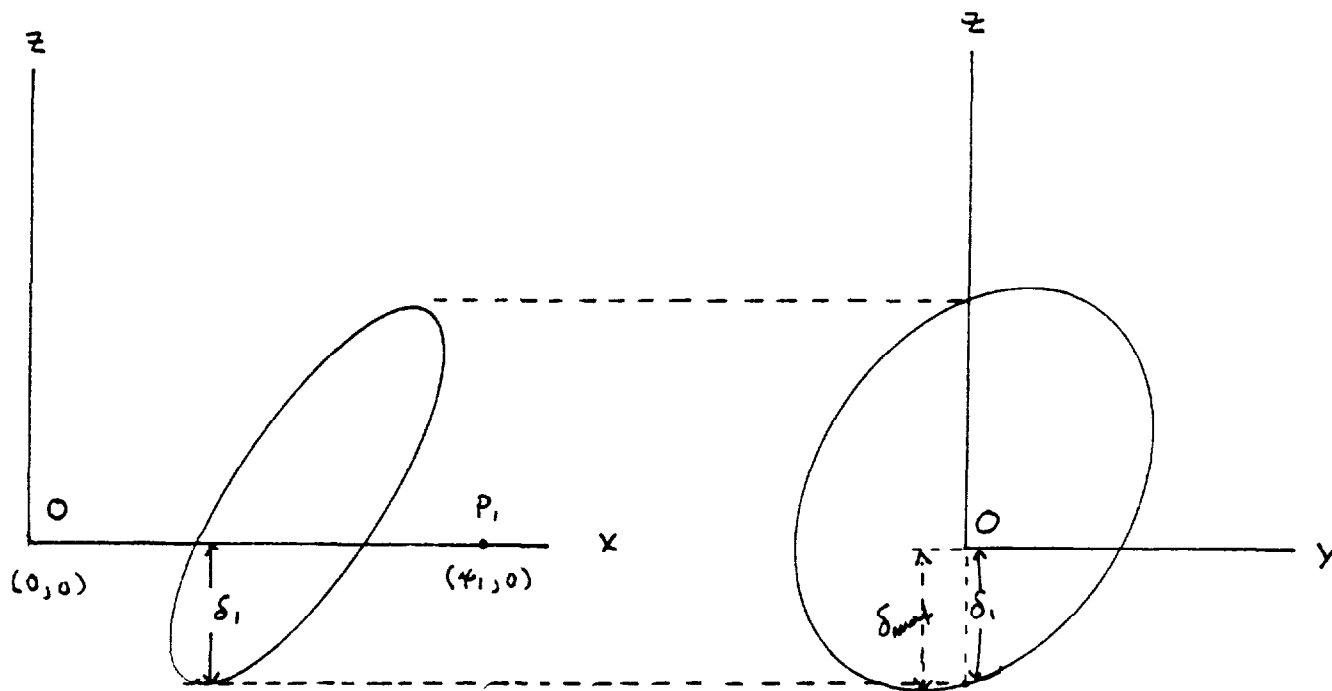


Figure 2a
x-z Intersection Ellipse

Figure 2b
y-z Projection Ellipse

Figure 2a shows the intersection of the ellipsoid and the x - z plane whereas figure 2b shows an orthographic projection of the ellipsoid onto the y - z plane so as to contrast δ_1 from δ_{\max} .

It may happen that the lowest point in the intersection of the ellipsoid with the x-z plane lies outside the panel boundary. One of these cases is illustrated in figure 3.

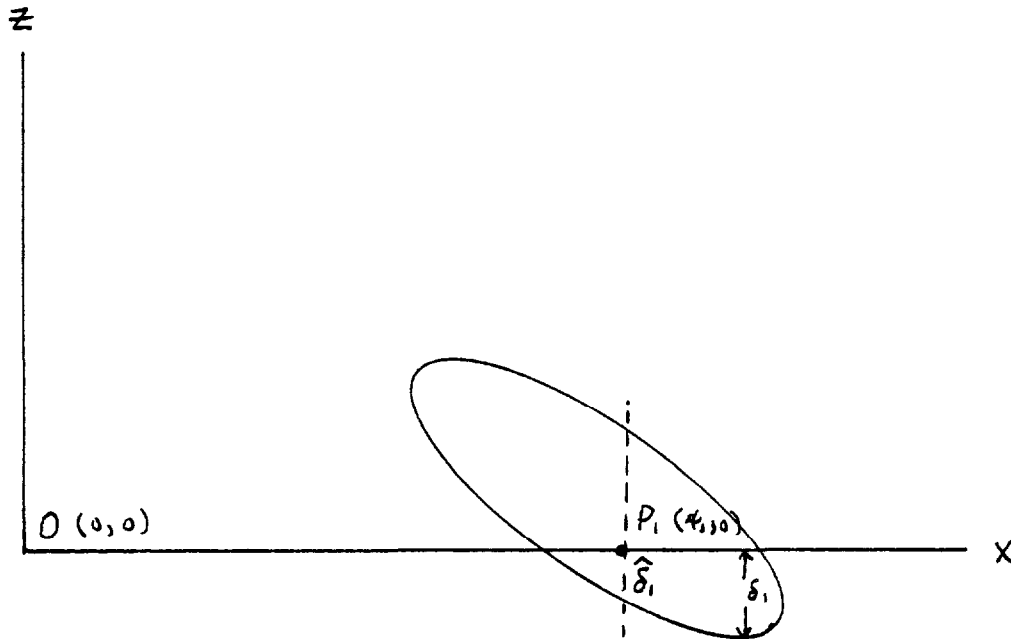


Figure 3 Minimum Above Panel Boundary

If the x-coordinate of the lowest point is greater than x_1 , then we define the edge penetration to be the distance from the panel surface to the point on the ellipse which is directly beneath $x_1: \hat{\delta}_1$. Similarly, if the x-coordinate of the lowest point is less than $x = 0$, as shown in figure 4, then we take as the edge penetration the distance from the panel surface to the point on the ellipse which is directly beneath $x=0: \hat{\delta}_0$.

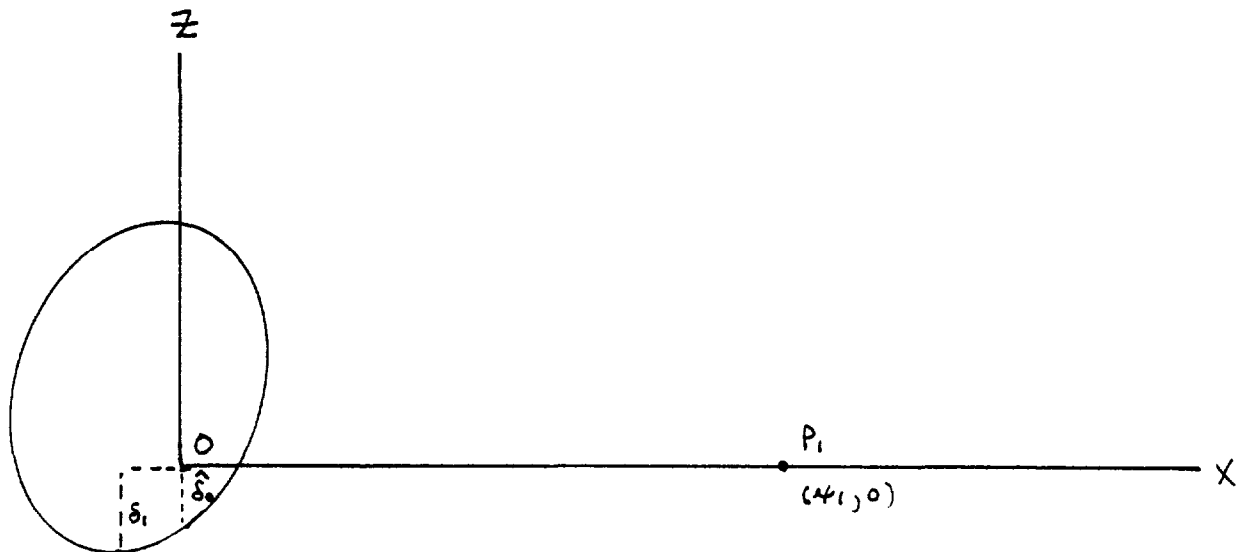
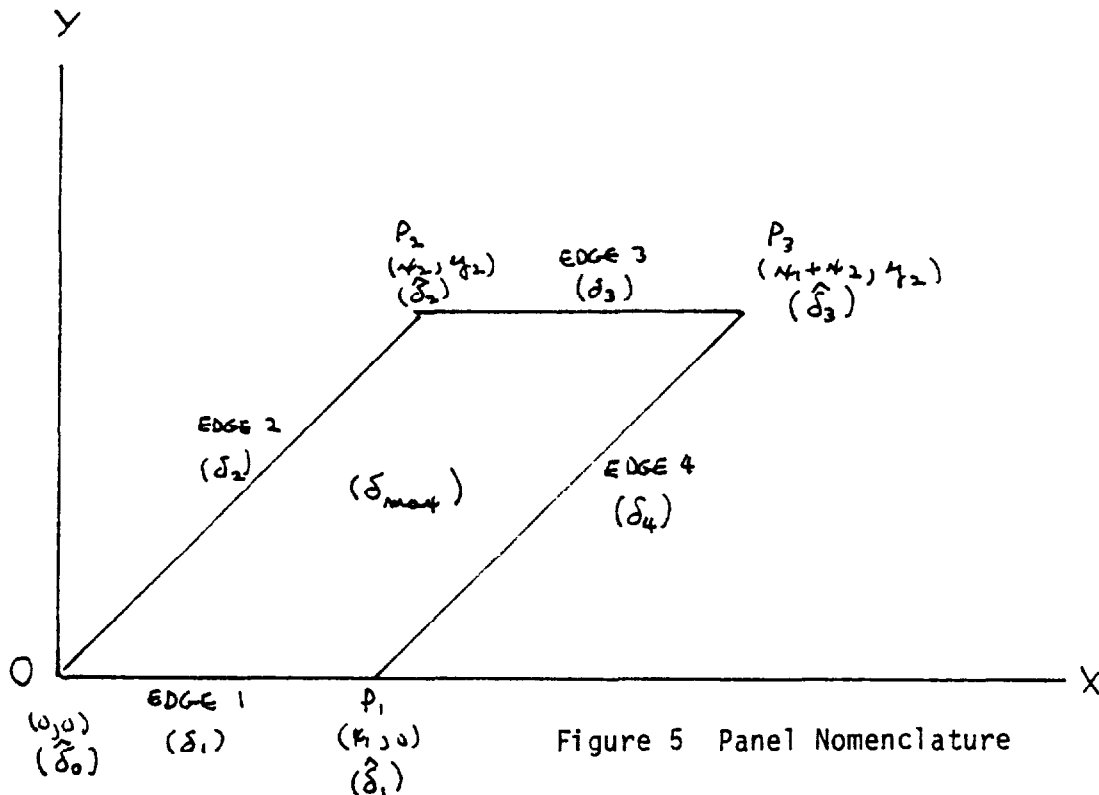


Figure 4 Minimum Below Panel Boundary

Thus, we see that the different types of penetrations which can arise, and for which we must derive expressions, are:

$$\delta_{max}, \delta_1, \delta_2, \delta_3, \delta_4, \hat{\delta}_0, \hat{\delta}_1, \hat{\delta}_2, \hat{\delta}_3$$

where the edges are defined in figure 5.



2.2 Calculation of Maximum Penetration for the Mid-Panel Case.

Recalling that the ellipsoid is

$$\frac{\xi^2}{a^2} + \frac{\eta^2}{b^2} + \frac{\zeta^2}{c^2} = 1$$

and the panel and ellipsoid systems are related by

$$\begin{pmatrix} \eta \\ \zeta \end{pmatrix} = D \begin{pmatrix} \xi \\ \zeta \end{pmatrix} + \begin{pmatrix} \eta_0 \\ \zeta_0 \end{pmatrix}$$

we find that the equation of the ellipsoid in the x, y, z system is

$$Ax^2 + By^2 + Cz^2 + Dx + Ey + Fz + Gx + Hy + Iz + J = 0$$

where

$$A = \frac{d_{11}^2}{a^2} + \frac{d_{12}^2}{b^2} + \frac{d_{13}^2}{c^2}$$

$$B = \frac{d_{21}^2}{a^2} + \frac{d_{22}^2}{b^2} + \frac{d_{23}^2}{c^2}$$

$$C = \frac{d_{31}^2}{a^2} + \frac{d_{32}^2}{b^2} + \frac{d_{33}^2}{c^2}$$

$$D = 2 \left(\frac{d_{11}d_{21}}{a^2} + \frac{d_{12}d_{22}}{b^2} + \frac{d_{13}d_{23}}{c^2} \right)$$

$$E = 2 \left(\frac{d_{11}d_{31}}{a^2} + \frac{d_{12}d_{32}}{b^2} + \frac{d_{13}d_{33}}{c^2} \right) \quad (4)$$

$$F = 2 \left(\frac{d_{21}d_{31}}{a^2} + \frac{d_{22}d_{32}}{b^2} + \frac{d_{23}d_{33}}{c^2} \right)$$

$$G = -2\gamma_0 \left(\frac{d_{11}^2}{a^2} + \frac{d_{12}^2}{b^2} + \frac{d_{13}^2}{c^2} \right) - 2\gamma_0 \left(\frac{d_{11}d_{21}}{a^2} + \frac{d_{12}d_{22}}{b^2} + \frac{d_{13}d_{23}}{c^2} \right) - 2\gamma_0 \left(\frac{d_{11}d_{31}}{a^2} + \frac{d_{12}d_{32}}{b^2} + \frac{d_{13}d_{33}}{c^2} \right)$$

$$H = -2\gamma_0 \left(\frac{d_{21}^2}{a^2} + \frac{d_{22}^2}{b^2} + \frac{d_{23}^2}{c^2} \right) - 2\gamma_0 \left(\frac{d_{11}d_{21}}{a^2} + \frac{d_{12}d_{22}}{b^2} + \frac{d_{13}d_{23}}{c^2} \right) - 2\gamma_0 \left(\frac{d_{21}d_{31}}{a^2} + \frac{d_{22}d_{32}}{b^2} + \frac{d_{23}d_{33}}{c^2} \right)$$

$$I = -2\gamma_0 \left(\frac{d_{31}^2}{a^2} + \frac{d_{32}^2}{b^2} + \frac{d_{33}^2}{c^2} \right) - 2\gamma_0 \left(\frac{d_{11}d_{31}}{a^2} + \frac{d_{12}d_{32}}{b^2} + \frac{d_{13}d_{33}}{c^2} \right) - 2\gamma_0 \left(\frac{d_{21}d_{31}}{a^2} + \frac{d_{22}d_{32}}{b^2} + \frac{d_{23}d_{33}}{c^2} \right)$$

$$J = \gamma_0^2 \left(\frac{d_{11}^2}{a^2} + \frac{d_{12}^2}{b^2} + \frac{d_{13}^2}{c^2} \right) + \gamma_0^2 \left(\frac{d_{21}^2}{a^2} + \frac{d_{22}^2}{b^2} + \frac{d_{23}^2}{c^2} \right) + \gamma_0^2 \left(\frac{d_{31}^2}{a^2} + \frac{d_{32}^2}{b^2} + \frac{d_{33}^2}{c^2} \right) + 2\gamma_0\gamma_0 \left(\frac{d_{11}d_{21}}{a^2} + \frac{d_{12}d_{22}}{b^2} + \frac{d_{13}d_{23}}{c^2} \right) + 2\gamma_0\gamma_0 \left(\frac{d_{11}d_{31}}{a^2} + \frac{d_{12}d_{32}}{b^2} + \frac{d_{13}d_{33}}{c^2} \right) + 2\gamma_0\gamma_0 \left(\frac{d_{21}d_{31}}{a^2} + \frac{d_{22}d_{32}}{b^2} + \frac{d_{23}d_{33}}{c^2} \right) - 1$$

The coordinates of the lowest point of the ellipsoid can be determined as follows. The intersection of the ellipsoid with the $z = -\delta$ plane forms an ellipse which has the equation

$$Ax^2 + By^2 + Dx + (G-E\delta)x + (H-F\delta)y + J - I\delta + C\delta^2 = 0 \quad (5)$$

By performing a suitable translation and rotation, it is possible to reduce this equation to the canonical form

$$\frac{\bar{x}^2}{\bar{a}^2} + \frac{\bar{y}^2}{\bar{b}^2} = 1 \quad (6)$$

Now δ_{\max} is determined by finding the value of δ for which \bar{a} and \bar{b} vanish and this happens if and only if

$$\begin{aligned} & (AF^2 + BE^2 - DEF + D^2C - 4ABC) \delta_{\max}^2 \\ & + (DEH - 2AFH + DFG - 2BEG + 4ABI - D^2I) \delta_{\max} \\ & + (AH^2 + BG^2 - DGH + D^2J - 4ABJ) = 0 \end{aligned} \quad (7)$$

The appropriate root of the quadratic is easily identified and we have

$$\begin{aligned} \delta_{\max} = & \frac{1}{(2AF - DE)F + (2BE - DF)E + 2(D^2 - 4AB)C} \cdot \\ & \left\{ (2AF - DE)H + (2BE - DF)G + (D^2 - 4AB)I \right. \quad (8) \\ & - \left[\left((2AF - DE)H + (2BE - DF)G + (D^2 - 4AB)I \right)^2 \right. \\ & \left. \left. - \left((2AF - DE)F + (2BE - DF)E + 2(D^2 - 4AB)C \right) \left((2AH - DG)H + (2BG - DH)G + 2(D^2 - 4AB)J \right) \right]^{1/2} \right\} \end{aligned}$$

The ellipsoid intersects the $z = -\delta_{\max}$ plane at the point with the coordinates

$$x_{\max} = \frac{2BG - DH - (2BE - DF)\delta_{\max}}{D^2 - 4AB} \quad (9)$$

$$y_{\max} = \frac{2AH - DG - (2AF - DE)\delta_{\max}}{D^2 - 4AB}$$

2.3 Penetration at Edge One

The intersection of the ellipsoid and the x-z plane is obtained by setting $y=0$.

$$Ax^2 + Cz^2 + Exz + Gx + Iz + J = 0 \quad (10)$$

The coordinates of the absolute minimum z value of this ellipse may be determined as follows. Setting $z = z_{\min}$ gives us the quadratic equation in x:

$$Ax^2 + (G + Ez_{\min})x + J + Iz_{\min} + Cz_{\min}^2 = 0 \quad (11)$$

The condition that (11) possesses a double root gives a quadratic equation in z_{\min}

$$(E^2 - 4AC)z_{\min}^2 + (2EG - 4AI)z_{\min} + G^2 - 4AJ = 0 \quad (12)$$

The root of this corresponding to the minimum is

$$z_{\min} = \frac{1}{E^2 - 4AC} \left\{ 2\sqrt{A} \sqrt{\frac{1}{2}(2AI - EG)I + \frac{1}{2}(2CG - EI)G + (E^2 - 4AC)J} + 2AI - EG \right\} \quad (13)$$

Also,

$$x_{\min} = -\frac{G + Ez_{\min}}{2A}$$

$$y_{\min} = 0$$

Now if $X_{\min} \geq X_1$ as pictured in Figure 3, z_{\min} satisfies

$$C z_{\min}^2 + (I + E X_1) z_{\min} + J + G X_1 + A X_1^2 = 0 \quad (14)$$

and we find

$$z_{\min} = \frac{-(E X_1 + I) - \sqrt{(E^2 - 4AC) X_1^2 - 2(2CG - EI) X_1 + I^2 - 4CJ}}{2C} \quad (15)$$

If on the other hand, $X_{\min} \leq 0$ as pictured in Figure 4, z_{\min} satisfies

$$C z_{\min}^2 + I z_{\min} + J = 0 \quad (16)$$

and

$$z_{\min} = \frac{-I - \sqrt{I^2 - 4CJ}}{2C} \quad (17)$$

2.4 Penetration at a General Edge

We will next consider the penetration at an edge defined by $y = \alpha x + \beta$ in the panel system. It is convenient to define a coordinate system x', y' such that x' lies along the line $y = \alpha x + \beta$ with its origin at $(x_c, x_c + \beta)$. This will be termed the edge system as is illustrated in Figure 6.

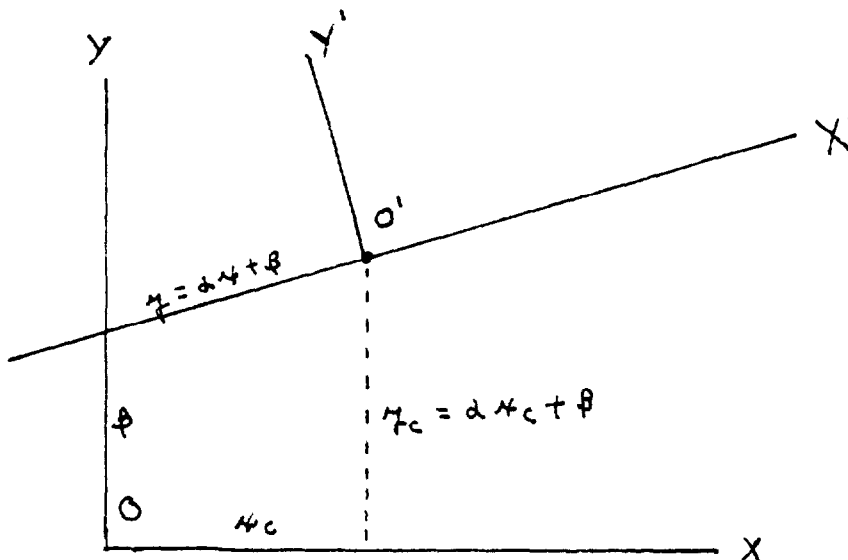


Figure 6 The Edge System

The two coordinate systems are related by

$$\begin{pmatrix} x' \\ y' \\ z' \end{pmatrix} = R \begin{pmatrix} x - x_c \\ y - y_c \\ z \end{pmatrix}$$

where

$$R = \begin{pmatrix} \frac{1}{\sqrt{1+d^2}} & \frac{d}{\sqrt{1+d^2}} & 0 \\ -\frac{d}{\sqrt{1+d^2}} & \frac{1}{\sqrt{1+d^2}} & 0 \\ 0 & 0 & 1 \end{pmatrix} \quad (18)$$

The relation between x', y', z' and ξ, η, ζ is

$$\begin{pmatrix} x' \\ y' \\ z' \end{pmatrix} = D' \begin{pmatrix} \xi \\ \eta \\ \zeta \end{pmatrix} + \begin{pmatrix} x'_0 \\ y'_0 \\ z'_0 \end{pmatrix} \quad (19)$$

where

$$D' = RD$$

and

$$\begin{pmatrix} x'_0 \\ y'_0 \\ z'_0 \end{pmatrix} = R \begin{pmatrix} x_0 - x_c \\ y_0 - y_c \\ z_0 \end{pmatrix} \quad (20)$$

Now previously we began with the relation

$$\begin{pmatrix} x \\ y \\ z \end{pmatrix} = D \begin{pmatrix} \xi \\ \eta \\ \zeta \end{pmatrix} + \begin{pmatrix} x_0 \\ y_0 \\ z_0 \end{pmatrix}$$

and we derived formulas for the penetration which results from the intersection of the ellipsoid with the $y = 0$ edge. Based upon this correspondence, we conclude that the formulas for the penetration which results from the intersection of the ellipsoid with the line $y = \alpha x + \beta$ is obtained by making the replacements

$$d_{ij} \rightarrow d'_{ij}, \quad x_0 \rightarrow x'_0, \quad y_0 \rightarrow y'_0, \quad z_0 \rightarrow z'_0$$

in the previous formulas. Once these coordinates are worked out, the coordinates with respect to the x, y, z system can be obtained by making use of the inverse transformation:

$$\begin{pmatrix} x \\ y \\ z \end{pmatrix} = R^T \begin{pmatrix} x' \\ y' \\ z' \end{pmatrix} + \begin{pmatrix} x_c \\ y_c \\ 0 \end{pmatrix} \quad (21)$$

Finally, the results for each of the panel edges is obtained by choosing appropriate values for α, β , and x_c .

2.5 Penetrations at Edges Two, Three, and Four

We present the results obtained from carrying out the method indicated in last section for the other three edges. It is convenient to begin by defining a series of quantities in order to shorten expressions.

Let

$$\begin{aligned} e_1 &= d_{11}^2 b^2 c^2 + d_{12}^2 a^2 c^2 + d_{13}^2 a^2 b^2 \\ e_2 &= d_{21}^2 b^2 c^2 + d_{22}^2 a^2 c^2 + d_{23}^2 a^2 b^2 \\ e_3 &= d_{31}^2 b^2 c^2 + d_{32}^2 a^2 c^2 + d_{33}^2 a^2 b^2 \\ e_{12} &= d_{11} d_{21} b^2 c^2 + d_{12} d_{22} a^2 c^2 + d_{13} d_{23} a^2 b^2 \\ e_{13} &= d_{11} d_{31} b^2 c^2 + d_{12} d_{32} a^2 c^2 + d_{13} d_{33} a^2 b^2 \\ e_{23} &= d_{21} d_{31} b^2 c^2 + d_{22} d_{32} a^2 c^2 + d_{23} d_{33} a^2 b^2 \\ \mu_1 &= a^2 M_{11}^2 + b^2 M_{12}^2 + c^2 M_{13}^2 \\ \mu_2 &= a^2 M_{21}^2 + b^2 M_{22}^2 + c^2 M_{23}^2 \\ \mu_3 &= a^2 M_{31}^2 + b^2 M_{32}^2 + c^2 M_{33}^2 \end{aligned} \quad (22)$$

$$\mu_{12} = a^2 M_{11} M_{21} + b^2 M_{12} M_{22} + c^2 M_{13} M_{23}$$

(22)

$$\mu_{13} = a^2 M_{11} M_{31} + b^2 M_{12} M_{32} + c^2 M_{13} M_{33}$$

(continued)

$$\mu_{23} = a^2 M_{21} M_{31} + b^2 M_{22} M_{32} + c^2 M_{23} M_{33}$$

where the $M_{i,j}$'s are minors of D.

In what follows, the discriminants of the various quadratic equations are given names Δ_i . Δ_i are so identified because they give information on the type of roots of the quadratic and therefore on conditions for contact between the ellipsoid and the panel edges. For example, let us consider Δ_1 .

If the x-z plane intersects the ellipsoid in an ellipse, then the ellipse will have an absolute minimum and an absolute maximum z value. These are obtained by solving a quadratic equation, the minimum corresponding to one root and the maximum corresponding to the other. If Δ_1 , the discriminant, is positive then these roots are different -- which means we have an ellipse. If Δ_1 is zero, then the roots are the same and the x-z plane contacts the ellipsoid at a single point. If Δ_1 is negative, the roots are imaginary and there is no intersection between the ellipsoid and the x-z plane.

Now we list the formulas for the remaining three edges. (Refer to figure 5).

Edge 2: If $0 \leq y_{\delta_2} \leq y_2$, we use

$$\delta_2 = -z_0 + \frac{1}{y_2^2 \mu_{22} + 2y_2 y_2 \mu_{12} + y_2^2 \mu_{11}} \quad (23)$$

$$\left[(y_2 \mu_{23} + y_2 \mu_{13})(y_0 y_2 - y_0 y_2) + \sqrt{y_2^2 e_1 + 2y_2 y_2 e_{12} + y_2^2 e_2} \sqrt{\Delta_4} \right]$$

where

$$y_{\delta_2} = \frac{y_2}{y_2^2 \mu_{22} + 2y_2 y_2 \mu_{12} + y_2^2 \mu_{11}} \left[(y_2 \mu_{22} + y_2 \mu_{12}) y_0 + (y_2 \mu_{12} + y_2 \mu_{11}) y_0 \right.$$

$$\left. + (y_2 e_{13} + y_2 e_{23}) \sqrt{\frac{\Delta_4}{y_2^2 e_1 + 2y_2 y_2 e_{12} + y_2^2 e_2}} \right]$$

and $\Delta_4 = y_2^2 \mu_{22} + 2y_2 y_2 \mu_{12} + y_2^2 \mu_{11} - (y_0 y_2 - y_0 y_2)^2 (\det D)^2$
 No contact with this edge if $\Delta_4 < 0$.

If $y_2 < y_{\delta_2}$, then we use

$$\hat{\delta}_2 = -z_0 + \frac{1}{e_3} \left[e_{13}(y_2 - y_0) + e_{23}(y_2 - y_0) + abc \sqrt{\Delta_5} \right]$$

where

$$\Delta_5 = e_3 - (\gamma_2 - \gamma_0)^2 \mu_1 - (\nu_2 - \nu_0)^2 \mu_2 - 2(\nu_2 - \nu_0)(\gamma_2 - \gamma_0) \mu_{1,2}$$

No contact with this edge if $\Delta_5 < 0$. If $y_{\delta 2} < 0$, then we use

$$\hat{\delta}_0 = -\gamma_0 + \frac{1}{e_3} \left(-\nu_0 e_{1,3} - \gamma_0 e_{2,3} + abc \sqrt{\Delta_3} \right) \quad (25)$$

where

$$\nu_{\delta 0} = 0$$

$$\gamma_{\delta 0} = 0$$

and

$$\Delta_3 = e_3 - \gamma_0^2 \mu_1 - 2\gamma_0 \nu_0 \mu_{1,2} - \nu_0^2 \mu_2$$

There is no contact with this edge if $\Delta_3 < 0$.

Edge 3. If $x_2 \leq x_{\delta 3} \leq x_1 + x_2$, then we use

$$\delta_3 = -\gamma_0 + \frac{1}{\mu_2} \left[\mu_{2,3} (\gamma_2 - \gamma_0) + \sqrt{e_1 \Delta_7} \right] \quad (26)$$

where

$$\nu_{\delta 3} = \nu_0 + \frac{1}{\mu_3} \left[-\mu_{1,2} (\gamma_2 - \gamma_0) + e_{1,3} \sqrt{\frac{\Delta_7}{e_1}} \right]$$

and

$$\Delta_7 = \mu_2 - (\gamma_2 - \gamma_0)^2 (\det D)^2$$

No contact with this edge if $\Delta_7 < 0$.

If $\nu_1 + \nu_2 < \nu_{\delta 3}$, then we use

$$\hat{\delta}_3 = -\gamma_0 + \frac{1}{e_3} \left[(\nu_1 + \nu_2 - \nu_0) e_{1,3} + (\gamma_2 - \gamma_0) e_{2,3} + abc \sqrt{\Delta_8} \right] \quad (27)$$

where

$$\Delta_8 = e_3 - (\gamma_2 - \gamma_0)^2 \mu_1 + (\nu_1 + \nu_2 - \nu_0)^2 \mu_2 - 2(\nu_1 + \nu_2 - \nu_0)(\gamma_2 - \gamma_0) \mu_{1,2}$$

No contact with this edge if $\Delta_8 < 0$.

If $x_{\delta_{\text{edge3}}} < x_2$, then we use δ_2 as defined previously.

There is no contact with this edge if $\Delta_5 < 0$.

Edge 4 If $0 \leq y_{\delta_4} \leq y_2$, then we use

$$\delta_4 = -z_0 + \frac{1}{\kappa_2^2 \mu_2 - 2\kappa_2 \gamma_2 \mu_{12} + \gamma_2^2 \mu_1} \cdot \left[(\kappa_2 \mu_{23} + \gamma_2 \mu_{13})(\kappa_0 \gamma_2 - \gamma_0 \kappa_2 - \kappa_1 \gamma_2) \right. \\ \left. + \sqrt{\kappa_2^2 e_1 + 2\kappa_2 \gamma_2 e_{12} + \gamma_2^2 e_2} \sqrt{\Delta_{10}} \right] \quad (28)$$

where

$$\gamma_{\delta_4} = \frac{\gamma_2}{\kappa_2^2 \mu_2 + 2\kappa_2 \gamma_2 \mu_{12} + \gamma_2^2 \mu_1} \left[(\kappa_2 \mu_2 + \gamma_2 \mu_{12})(\kappa_0 - \kappa_1) + (\gamma_2 \mu_1 + \kappa_2 \mu_{12}) \kappa_0 \right. \\ \left. + (e_{13} \kappa_2 + e_{23} \gamma_2) \sqrt{\frac{\Delta_{10}}{\kappa_2^2 e_1 + 2\kappa_2 \gamma_2 e_{12} + \gamma_2^2 e_2}} \right]$$

and

$$\Delta_{10} = \kappa_2^2 \mu_2 + 2\kappa_2 \gamma_2 \mu_{12} + \gamma_2^2 \mu_1 - (\kappa_0 \gamma_2 - \gamma_0 \kappa_2 - \kappa_1 \gamma_2)^2 (\det D)^2$$

No contact with this edge if $\Delta_{10} < 0$.

If $y_2 < y_{\delta_4}$, then we use δ_3 as defined previously.

There is no contact with this edge if $\Delta_8 < 0$.

If $y_{\delta_4} < 0$, then we use

$$\hat{\delta}_1 = -z_0 + \frac{1}{e_3} \left[(\kappa_1 - \kappa_0) e_{13} - \gamma_0 e_{23} + abc \sqrt{\Delta_2} \right] \quad (29)$$

where

$$\kappa_{p_1} = \kappa_1$$

$$\gamma_{p_1} = 0$$

and

$$\Delta_2 = e_3 - \gamma_0^2 \mu_1 + 2\gamma_0 (\kappa_1 - \kappa_0) \mu_{12} - (\kappa_1 - \kappa_0)^2 \mu_2$$

No contact if $\Delta_2 < 0$.

We also restate the results of Sections 2.2 and 2.3 in terms of this notation.

$$\delta_{\max} = -z_0 + \frac{\sqrt{\mu_3}}{\det D}$$

$$\nu_{\max} = \nu_0 - \frac{\mu_{13}}{\sqrt{\mu_3} \det D} \quad (30)$$

$$z_{\min} = y_0 + \frac{\mu_{23}}{\sqrt{\mu_3} \det D}$$

$$\delta_1 = -z_0 + \frac{1}{\mu_2} \left(\sqrt{e_1 \Delta_1} - y_0 \mu_{23} \right)$$

$$\nu_{\delta_1} = \nu_0 + \frac{1}{\mu_2} \left(e_{13} \sqrt{\frac{\Delta_1}{e_1}} + y_0 \mu_{12} \right)$$

$$y_{\delta_1} = 0$$

where

$$\Delta_1 = \mu_2 - y_0^2 (\det D)^2$$

2.6 Calculation of Edge Effects

When an ellipsoid approaches a planar panel from the side, the definitions of penetration in the previous sections can lead to a discontinuity in penetration when the tip of the ellipsoid intrudes below the panel. Figure 7 illustrates this situation.

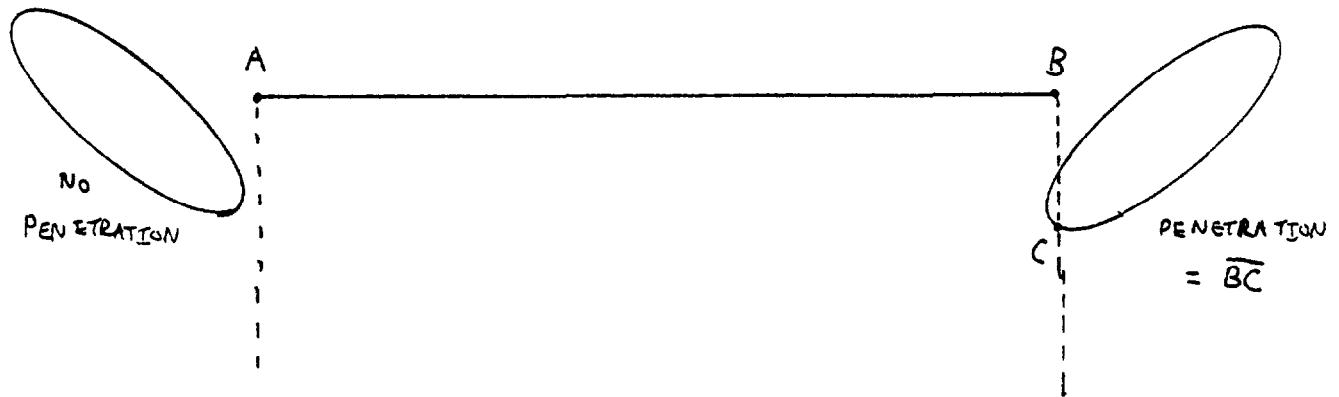


Figure 7. DISCONTINUITY AT EDGES

If the material is stiff, the resulting discontinuity in force can upset the tracking of the integration in a way which cutting down the integration time step will not be correct. In order to protect against this type of discontinuity, force is linearly scaled on as a function of the distance of the ellipsoid center from the panel edge which is closest.

The distance used to scale against is taken as the radius of the sphere which circumscribes the ellipsoid. The scaling is adjusted so the factor is .5 when the ellipsoid center lies over the dominating edge. Figure 8 illustrates the situation.

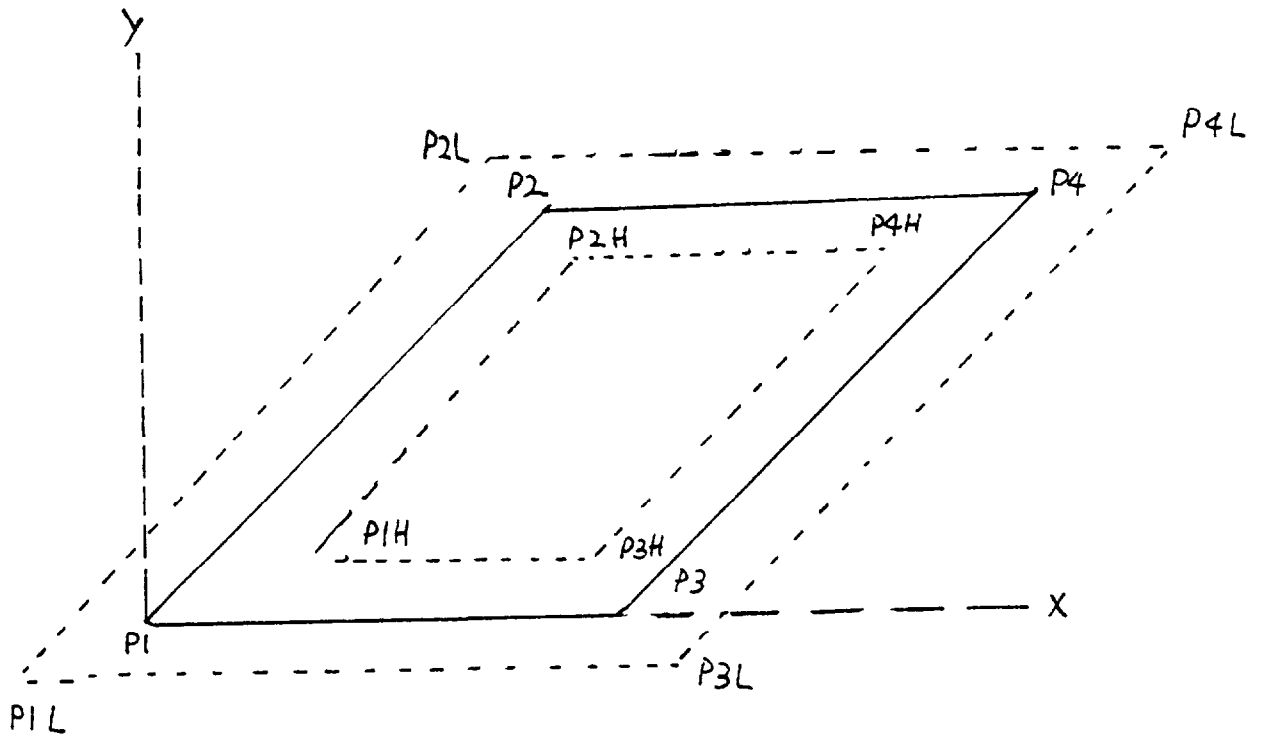


Figure 8. Edge Scaling Factor Zones

The Normal Force Scaling Factor (SF) is defined one when the ellipsoid center is over the full contact panel zone (P1H-P2H-P4H-P3H-P1H) and is zero when the ellipsoid center is outside the panel contact zone, (P1L-P2L-P4L-P3L-P1L). When the ellipsoid is within the panel contact zone and without the full contact panel zone, the Scaling Factor takes on a value between zero and one.

The Normal Force Scaling Factor is defined as

$$SF = \frac{1}{2} \max \left(0, \min \left(2, 1 + \frac{y_0}{\pi}, 1 + \frac{y_2 - y_0}{\pi}, \right. \right. \\ \left. \left. 1 + \frac{y_2 y_0 - y_2 y_0}{\varphi}, 1 + \frac{y_1 y_2 + y_2 y_0 - y_2 y_0}{\varphi} \right) \right) \quad (31)$$

where

(x_0, y_0, z_0) are the coordinates of the ellipsoid center in the panel system,

$(0, 0, 0)$ are the coordinates of point P1 in the panel system,

(31)

Continued

$(x_2, y_2, 0)$ are the coordinates of point P2 in the panel system,

$(x_1, 0, 0)$ are the coordinates of point P3 in the panel system,

$$Q = \bar{\pi} \sqrt{x_2^2 + y_2^2},$$

and

$\bar{\pi} = \max(a, b, c)$ See Section 2.1 for definitions of ellipsoid and panel system.

2.7 Tangential Forces

Many material panels resist motion along their surfaces as well as motion into their surfaces. Two types of tangential resistance are approximated in this model: Coulomb Friction and "Snapback" Force.

The Coulomb friction is defined as:

$$F_{CF} = (\mu_0 + \mu_1 \delta + \mu_2 \delta^2) F_N \min\left(\frac{|\dot{x}|}{v}, 1\right)$$

(32)

where

μ_0, μ_1, μ_2 are the inputted friction coefficients,
 δ is the penetration,
 F_N is the normal force due to load-deflection,
 \dot{x} is the tangential velocity along face of panel,

and

v is the inputted velocity threshold for full friction.

(32)

Continued

The Snapback force deals with the "piling up" of panel material in front of the ellipsoid as it continues across the panel surface and is defined as

$$F_{SB} = a_1 \bar{\delta} + a_2 \bar{\delta}^2$$

(33)

where

a_1, a_2 are the inputted snapback coefficients,

and

$\bar{\delta}$ is the distance along the face of the panel from the point of contact.

Coulomb friction and Snapback force are combined to form total tangential force which is scaled to ramp on force for fast moving ellipsoids, is also scaled for edge effects, and is also subject to an absolute maximum.

$$F_T = \min \left(\min(\delta, 2r_{ez}) S (F_{cF} + F_{SB}), F_{Tmax} \right)$$

where

(34)

$$S = \max \left(0, \min \left(1, \frac{y_0}{r}, \frac{y_2 - y_0}{r}, \frac{y_2 y_0 - y_0 y_0}{Q}, \frac{r_1 y_2 + y_2 y_0 - y_2 y_0}{Q} \right) \right),$$

r_{ez} is the distance from the ellipsoid center and the lowest point of the ellipsoid in the panel system,

F_{Tmax} is the inputted maximum tangential force, and all other quantities as previously defined.

2.8 Recognition of Being Behind the Panel

There are many circumstances in which an ellipsoid may be positioned behind a panel without having penetrated through the panel (e.g., the feet underneath the steering wheel or the dash). Automatic recognition of this situation is handled initially by the simple criteria of whether the ellipsoid breaks the plane of the panel and whether it has a non-zero penetration as defined in the previous sections. If both criterion are met, the intrusion is defined to be from the front. In succeeding times, the state of being behind or coming from the front is remembered in a switch maintained for each interaction. The switch is modified back to the initial condition if ellipsoid totally lies above the panel plane or goes out of contact to the side of the panel.

2.9 Calculation of Solid Corner Effects

It is possible to designate that any panel is the face of a solid. In this case, normal edge scaling is replaced with special corner scaling when an ellipsoid is deemed to be following the solid round the corner. If the user does not so designate a panel, then scaling is applied as explained above. Figure 9 illustrates a typical solid corner with an ellipsoid moving around the corner. If these two panels are treated ac-

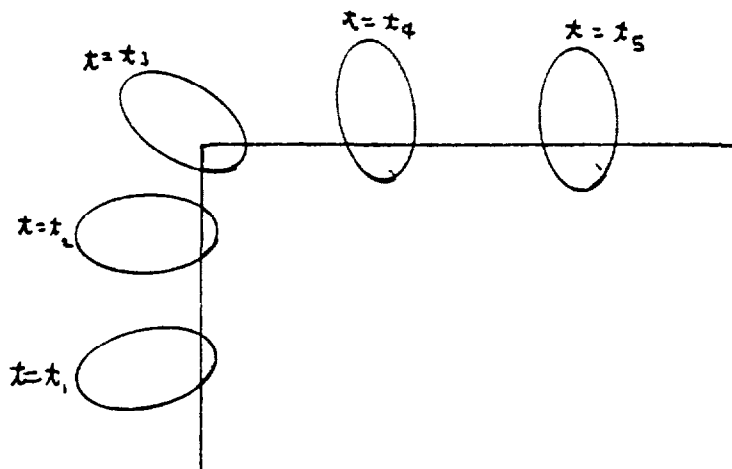


Figure 9. The Solid Corner Situation

According to the rules of the previous sections, at the first two times, the ellipsoid will be in full contact with Panel 2 and be behind Panel 1. At time t_3 , edge scaling will reduce the ellipsoid contact with Panel 2 and still no contact with Panel 1. At the last two times, we would see increasing force due to Panel 2 and still no contact with Panel 1.

The Solid Corner Effect would produce non-zero force due only to Panel 2 at the first two times, due to both panels at t_3 and due only to Panel 1 at the last two times.

For programming convenience, an additional requirement is made that the algorithm required to apply to each panel separately without knowledge of the other panel(s) forming the solid corner. An enabling assumption is made that the unknown panel(s) lie at right angles to the panel under consideration.

$$SCF = \frac{z_0 + \bar{\pi}}{\sqrt{(x_0 - \bar{\pi})^2 + (y_0 - \bar{\pi})^2 + (z_0 + \bar{\pi})^2}} \quad (35)$$

where

x_0, y_0, z_0 are the coordinates of the ellipsoid center in panel system,

and

$\bar{\pi}$ is the maximum semiaxis length of the ellipsoid.

Figure 10 illustrates the situation.

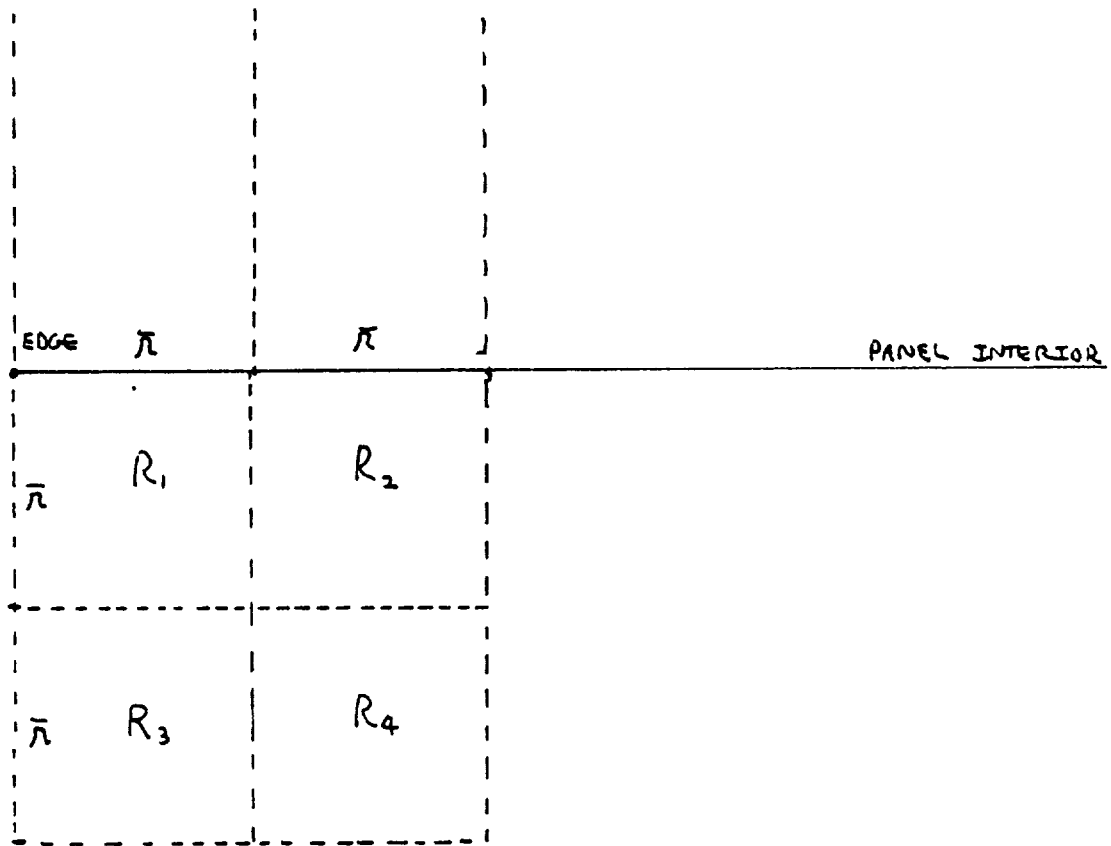


Figure 10. Panel Treated as Part of Solid Corner

The SCF is applied in addition to the edge scaling factors. The control regions shown in Figure 10 are used to turn on and shut off computation of SCF depending on the previous events. The current state and previous history of a contact interaction is recorded by means of the values assigned to a set of "state" switches, the details of which will not concern us here.

Referring to Figure 10, when an ellipsoid has been in contact with the interior of a panel which has been designated part of a solid corner and the center of the ellipsoid makes its way into R_1 or lies above R_1 , then normal edge scaling is used. When an ellipsoid center enters R_3 , normal edge scaling continues as long as deflection is not increasing, but when deflection increases, corner scaling begins in addition to edge scaling. When the ellipsoid center passes below R_3 , the ellipsoid is considered behind the panel. When an ellipsoid has been behind the panel and its center passes into R_1 , motion towards the midpoint of the panel is monitored. If motion is away from the midpoint, the ellipsoid is still considered behind the panel. If the motion is towards the midpoint then corner scaling is used until the ellipsoid center crosses into R_2 when the contact is considered to be interior from the top (full on). A similar computation is used for each of the other panels forming the solid corner when they are separately considered.

3.0 Load-Deflection Properties

Ellipsoids and Panels each can have load-deflection properties specified by the user. This section describes the characteristics which it is possible to ascribe to ellipsoids and panels. The five following sections deal with loading characteristics, unloading characteristics, reloading characteristics, bivariate tables, saturation and breakdown.

3.1 Loading Characteristics

Three general classes of loading curves are allowed. First is the bivariate polynomial. Second is the bivariate table. Third is null or zero properties.

The bivariate polynomial is of the form

$$F = \sum_{\substack{0 \leq i, j \leq 6, \\ 0 < i+j \leq 6}} a_{ij} \delta^i \dot{\delta}^j \quad (36)$$

of which at least one a_{ij} must be non-zero.

There are a maximum of twenty-seven such terms which may be used to describe polynomials up to a homogeneous equation of degree six (case when $i + j = 6$).

The random bivariate table can be described as a set of triples $(\delta_i, \dot{\delta}_i, F_i)$ for $i = 1, \dots, N$ where N is at least four. Tables may also be specified on a fixed lattice and/or with dependence on only deflection or deflection rate alone. A succeeding section discusses the approach taken to interpolation in each of these cases.

The null possibility enables some special effect such as tangential resistance coupled with no normal resistance to simulate "wind".

3.2 Unloading Characteristics

Four basic types of unloading characteristics are provided. The first type is unloading back down the loading curve. If the loading curve contains rate dependence then a hysteresis effect can be simulated in this way. It is also possible to specify "elastic behavior as a

variation in which only the magnitude of rate is used in computing rate terms. The second type is unloading down a bilinear curve computed from G and R ratios. The third type is unloading down a linear curve of specified slope. The fourth type is unloading down a linear curve computed using only the G ratio.

The G ratio is defined as the ratio of permanent deformation to deformation beyond previous permanent deformation. $G = 0$ represents a completely resilient material. The R ratio is defined as the ratio of conserved energy upon complete unloading to potential energy at turnaround. $R = 1$ describes a completely energy-efficient material. The G and R ratios are not completely independent and it is the users responsibility to maintain an appropriate relationship between the two. Either G and/or R may be specified as a constant or as a tabular function of turnaround deflection. Clearly the following two inequalities must always be satisfied.

$$0 \leq G < 1 \quad \text{and} \quad 0 < R \leq 1 \quad (37)$$

The turnaround deflection (Ω) is defined as that deflection for which deflection rate is zero. This deflection is approximated from the current deflection and deflection rate together with the last two such pairs.

$$\begin{aligned} \Omega = & \left(\frac{\dot{\delta}_{-1}}{\dot{\delta}_{-2} - \dot{\delta}_0} \right) \left(\frac{\dot{\delta}_{-2}}{\dot{\delta}_{-1} - \dot{\delta}_0} \right) \delta_0 - \left(\frac{\dot{\delta}_0}{\dot{\delta}_{-2} - \dot{\delta}_{-1}} \right) \left(\frac{\dot{\delta}_{-2}}{\dot{\delta}_{-1} - \dot{\delta}_0} \right) \delta_{-1} \\ & + \left(\frac{\dot{\delta}_0}{\dot{\delta}_{-2} - \dot{\delta}_{-1}} \right) \left(\frac{\dot{\delta}_{-1}}{\dot{\delta}_{-2} - \dot{\delta}_0} \right) \delta_{-2} \end{aligned} \quad (38)$$

where

- $\delta_0, \dot{\delta}_0$ are deflection and deflection rate at current time step
- $\delta_{-1}, \dot{\delta}_{-1}$ are deflection and deflection rate at last previous time step
- $\delta_{-2}, \dot{\delta}_{-2}$ are deflection and deflection rate at next to last previous time step

If any of the denominators in (38) vanish then

$$\underline{\Omega} = \max(\delta_0, \delta_{-1}, \delta_{-2}) \text{ is used.} \quad (39)$$

Permanent deformation and conserved energy are computed using

$$\begin{aligned} \omega_0 &= G(\Omega - \omega_{-1}), \\ E_c &= R E \end{aligned} \quad (40)$$

where

ω = permanent deformation
 E = current potential energy

If bilinear unloading is being used then

$$\begin{aligned} \Delta &= \Omega - \frac{E_c}{\hat{F}}, \\ \alpha_1 &= \frac{E_c \hat{F}}{\hat{F}(\Omega - \omega) - E_c}, \\ \beta_1 &= -\alpha_1 \omega, \\ \alpha_2 &= \frac{\hat{F}^2}{\alpha_1}, \\ \beta_2 &= \hat{F} - \alpha_2 \Omega \end{aligned} \quad (41)$$

where

\hat{F} is force value at turnaround deflection

$\gamma = \frac{\hat{F}}{\Omega - \omega}$ = unloading slope for straight line from turnaround to permanent deflection

Δ is the changeover deflection

α_1, β_1 are coefficients of lower linear segment

α_2, β_2 are coefficients of upper linear segment

and unloading force is defined as

$$F_u = \begin{cases} \alpha_1 \delta + \beta_1 & \text{if } \omega \leq \delta \leq \Delta \\ \alpha_2 \delta + \beta_2 & \text{if } \Delta \leq \delta \leq \Omega \end{cases}$$

If linear unloading based on G ratio alone is being used then

$$F = \alpha \delta + \beta, \quad \omega \leq \delta \leq \Omega$$

where

$$\alpha = \gamma,$$

$$\text{and } \beta = -\gamma \omega$$

(42)

If linear unloading based on slope is being used then

$$F = \alpha \delta + \beta, \quad \omega \leq \delta \leq \Omega$$

where

$$\alpha = \text{inputted slope},$$

$$\beta = -\alpha \omega,$$

$$\text{and } \omega = \Omega - \frac{\hat{F}}{\alpha}.$$

(43)

3.3 Reloading Characteristics

Two basic types of reloading characteristics are provided. Regular reloading scales on deflection up to the corresponding force at the maximum deflection and the current deflection rate. Alternate reloading uses the original loading curve pushed so that the zero point corresponds to the permanent deformations.

The equation used for regular reloading is as follows:

$$F = \frac{(\delta - \bar{\omega}) \tilde{F} + (\Omega - \delta) \bar{F}}{\Omega - \bar{\omega}}$$

$$\frac{\partial F}{\partial \delta} = \frac{\hat{F} - \bar{F}}{\Omega - \bar{\omega}} \quad (44)$$

$$\frac{\partial F}{\partial \dot{\delta}} = \left(\frac{\delta - \bar{\omega}}{\Omega - \bar{\omega}} \right) \frac{\partial \tilde{F}}{\partial \dot{\delta}}$$

where

$\bar{\omega}$ is the deflection at which unloading changes to reload, the minimum value

\bar{F} is the unloading force at $\bar{\omega}$

\tilde{F} is a generalization of \hat{F} obtained by loading force evaluation with $\delta = \Omega$ and $\dot{\delta}$ = current $\dot{\delta}$

Equation (44) then linearly scales from the turnaround point $(\bar{\omega}, 0)$ in the $\delta, \dot{\delta}$ plane to the point along the $\delta = \Omega$ line corresponding to the current value of deflection rate. This scaling has the property of producing continuous forces with the resumption of the loading curve when $\delta > \Omega$.

Alternative reloading simply evaluates force as $F(\delta - \bar{\omega}, \dot{\delta})$.

3.4 Bivariate Table Interpolation

The most general form of table available is a random set of triples $(\delta_i, \dot{\delta}_i, F_i)$ for $i = 1$ to N . In the input section, a lattice of boxes

is set up in the δ - $\dot{\delta}$ plane and the triples are sorted into boxes. When interpolating for an arbitrary point $(\delta, \dot{\delta})$, a search starts in the box containing $(\delta, \dot{\delta})$ and then continues in increasing surrounding tiers until the three closest points are identified. A planar interpolation is then done using those three points. If the input is given for a regular or irregular lattice in δ - $\dot{\delta}$ plane then the lattice box is found containing the $(\delta, \dot{\delta})$ and computed with linear interpolations along the top, bottom, and the vertical line containing the point.

$$F = q_2 F_L + p_2 F_u \quad (45)$$

where

$$p_2 = \frac{\dot{\delta} - \dot{\delta}_0}{\dot{\delta}_1 - \dot{\delta}_0}, \quad F_L = q_1 F_1 + p_1 F_2,$$

$$q_2 = \frac{\dot{\delta}_1 - \dot{\delta}}{\dot{\delta}_1 - \dot{\delta}_0} = 1 - p_2, \quad F_u = q_1 F_3 + p_1 F_4,$$

$$p_1 = \frac{\delta - \delta_0}{\delta_1 - \delta_0}, \quad q_1 = \frac{\delta_1 - \delta}{\delta_1 - \delta_0} = 1 - p_1$$

and the four corners of the lattice box are $(\delta_0, \dot{\delta}_0, F_1)$, $(\delta_1, \dot{\delta}_0, F_2)$, $(\delta_0, \dot{\delta}_1, F_3)$, $(\delta_1, \dot{\delta}_1, F_4)$.

Bivariate tables can be also simplified to tables in deflection or deflection rate alone. If this is the case, piecewise linear interpolation is used and only pairs are stored (δ_i, F_i) or $(\dot{\delta}_i, F_i)$ as applicable.

3.5 Saturation and Breakdown

Saturation is a force maximizing. The normal definition of loading force is modified

$$F = \begin{cases} F_L & \text{when } F < F_S, \\ F_S & \text{otherwise} \end{cases} \quad (46)$$

where F_L is normal loading force,

and F_S is inputted saturation force.

If force is not saturated all normal unloading and reloading options exist as described in previous sections.

If force is saturated then unloading and reloading is governed by a straight line which is computed either as slope unloading or G-unloading.

$$F = \begin{cases} F_s & \text{if } \delta > \Omega \\ F_s \left(\frac{\delta - \omega}{\Omega - \omega} \right) & \text{if } \Omega \geq \delta \geq \omega \\ 0 & \text{if } \delta < \omega \end{cases} \quad (47)$$

where

$$\omega = -G_s (\Omega - \delta_c) \quad \text{if } G_s < 0,$$

or

$$\omega = \Omega - \frac{F_s}{G_s} \quad \text{if } G_s > 0,$$

F_s is inputted saturation force,

G_s is inputted saturation slope,

and δ_c is the yield deflection.

Breakdown occurs when deflection increases beyond the breakdown point. Breakdown supercedes all other loading options including saturation. Breakdown proceeds linearly from the force obtained at the breakdown point to zero at the breaking point. Once the breaking point is reached, no further force will be generated under any circumstances. If unloading occurs, the regular unloading options specified is used. If reloading occurs, it is linear from the unloading force at the turnaround deflection at the maximum deflection reached in breakdown loading. Beyond that point, breakdown loading resumes.

Breakdown loading is

$$F = \frac{F_D}{\delta_F - \delta_D} (\delta_F - \delta), \quad \delta_D \leq \delta \leq \delta_F \quad (48)$$

where

δ_D is inputted breakdown deflection

F_D is loading force at δ_D and current δ

δ_F is inputted breaking or failure point

Reloading to breakdown is

$$F = \frac{\hat{F} - \bar{F}}{\Omega - \bar{\omega}} (\delta - \bar{\omega}) + \bar{F}, \quad \bar{\omega} \leq \delta \leq \Omega, \quad \delta_D \leq \Omega \leq \delta_F \quad (49)$$

where previous definitions apply.

4.0 Shared Deflection

When two physical bodies are pushed together, both will deform. Figure 11 illustrates the situation. The shared deflection algorithms approximate the amount of deformation of each body. Let us define $\Delta(\delta, \dot{\delta})$, the force imbalance function as

$$\Delta(\delta, \dot{\delta}) = F(\delta_1, \dot{\delta}_1) - G(\delta_2, \dot{\delta}_2) \quad (50)$$

where

$F(\delta_1, \dot{\delta}_1)$ = force function for first body

$G(\delta_2, \dot{\delta}_2)$ = force function for second body

$\delta_1, \dot{\delta}_1$ are deflection and deflection rate for first body

$\delta_2, \dot{\delta}_2$ are deflection and deflection rate for second body

The shared deflection problem can then be stated: given $\delta, \dot{\delta}$ find $\delta_1, \dot{\delta}_1, \delta_2, \dot{\delta}_2$ such that

$$1. \quad \Delta(\delta_1, \dot{\delta}_1) = 0$$

$$2. \quad \delta_1 + \delta_2 = \delta, \quad 0 \leq \delta, \delta_1, \delta_2 \quad (51)$$

$$3. \quad \dot{\delta}_1 + \dot{\delta}_2 = \dot{\delta}$$

Since δ and $\dot{\delta}$ are functions of the overall problem, in general (51) can not even be written. The approach taken is to set up one or more new problems at each new time step based on current values of δ , and $\dot{\delta}$ and applicable forms of F and G and then require continuity of $\delta_1, \dot{\delta}_1, \delta_2$, and $\dot{\delta}_2$ with past values of these quantities. Viewed in this light, the problem becomes one or more highly non-linear first order differential equations in δ_1 . The multiple equations come from the loading-unloading-reloading options previously explained which F and G depending on ranges in $\delta_1, \dot{\delta}_1, \delta_2$, and $\dot{\delta}_2$.

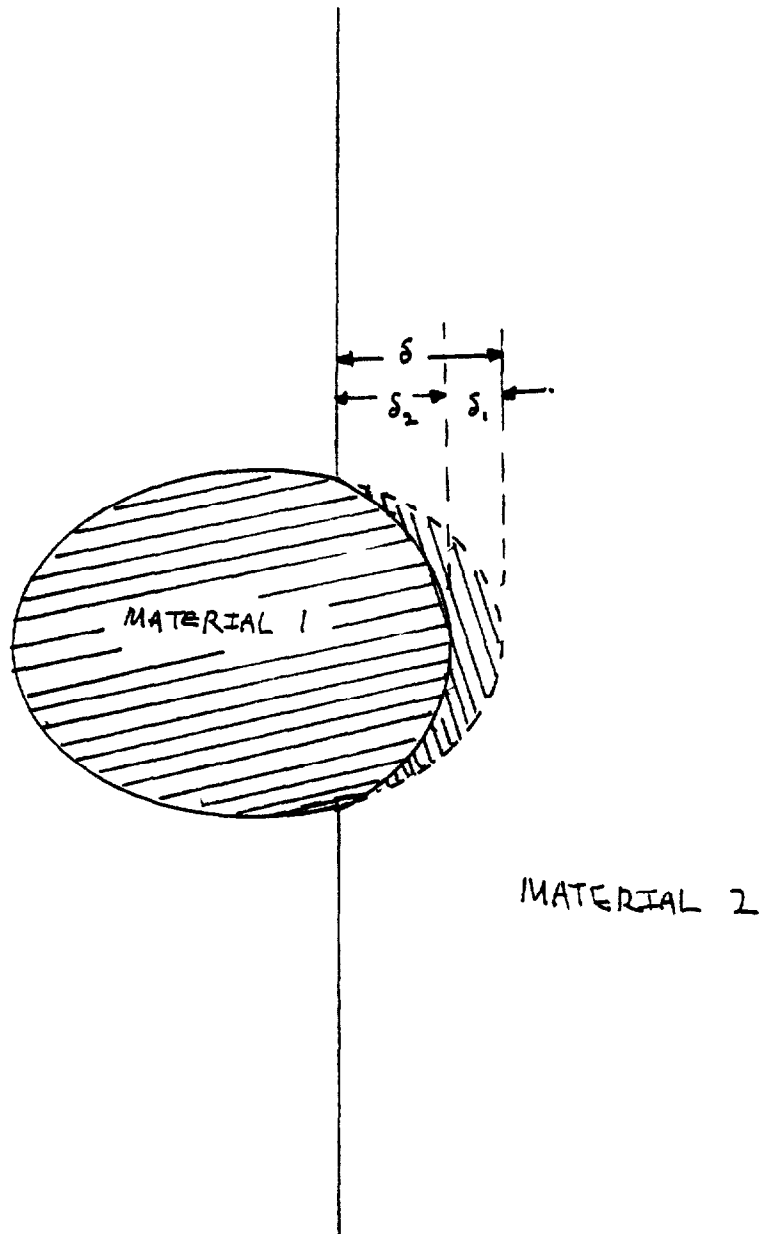


Figure 11. Mutual Deformation of an
Ellipse on a Line

A general interactive procedure was developed and is presented in the next section. An algorithm for the special case when both F and G are first order in both deflection and deflection rate is taken up in the next sub section. The next section discusses the situation when both F and G are sixth order polynomials in pure deflection or pure deflection rate. The next subsection deals with the general function of deflection alone. The final subsection deals with the case when F or G or both are bivariate tables.

This multiplicity of approaches was dictated by the gross simplifications necessary to get even a crude approximation to the solution for this problem.

4.1 General Algorithm

If Δ is considered a function of δ_1 and $\dot{\delta}_1$ alone and is plotted over the $\delta_1-\dot{\delta}_1$ plane, then $\Delta(\delta_1, \dot{\delta}_1)=0$ is a closed contour which changes shape from one time step to the next. Only one point on this contour is correct for the physical condition and the materials involved. The general algorithm is designed to find the contour and then follow it around until the appropriate point on the contour is found. This is a two step process.

The first step starts with the solution found at the last time step on the old contour and extrapolates in time to the new contour.

$$\dot{\delta}_i = \dot{\delta}_{ip} + \frac{\frac{\partial G}{\partial \delta_p} (\delta - \delta_p) + \frac{\partial G}{\partial \dot{\delta}_p} (\dot{\delta} - \dot{\delta}_p) + 2 \frac{\partial F}{\partial \dot{\delta}_p} \dot{\delta}_{ip}}{\frac{\partial F}{\partial \dot{\delta}} + \frac{1}{2} \Delta t \frac{\partial F}{\partial \delta}}$$

$$\delta_i = \delta_{ip} + \frac{1}{2} \Delta t \left(\dot{\delta}_i - \dot{\delta}_{ip} \right) \quad (52)$$

where

$\delta, \dot{\delta}$ are the combined deflection and deflection rate,

$\delta_p, \dot{\delta}_p$ are the combined deflection and deflection rate at the last time step,

Δt is the time step,

and

$\frac{\partial F}{\partial \delta_p}, \frac{\partial F}{\partial \dot{\delta}_p}, \frac{\partial G}{\partial \delta_p}, \frac{\partial G}{\partial \dot{\delta}_p}$ are the corresponding partials evaluated at the last time step.

The second step in the general procedure involves trying to improve the solution by moving around the contour to find the point that fits.

This is achieved by combining the expression for zero differential of Δ with a first order continuity expression.

$$\dot{\delta}_j = \frac{\frac{\partial \Delta_i}{\partial \delta_i} (\delta_{i,i} - \delta_{i,p} - \frac{1}{2} \Delta t (\dot{\delta}_{i,i} + \dot{\delta}_{i,p})) - \Delta \dot{i}}{\frac{1}{2} \Delta t \frac{\partial \Delta_i}{\partial \delta_i} + \frac{\partial \Delta_i}{\partial \dot{\delta}_i}} \quad (53)$$

$$\delta_j = \frac{-\Delta_i - \frac{\partial \Delta_i}{\partial \dot{\delta}_i} \dot{\delta}_j}{\frac{\partial \Delta_i}{\partial \delta_i}}$$

where

the i subscript denotes the iteration being stepped off from,

the j subscript denotes the iteration being computed,

the p subscript denotes a value from the last time step,

$$\frac{\partial \Delta}{\partial \delta_i} = \frac{\partial F}{\partial \delta_i} + \frac{\partial G}{\partial \delta_i},$$

and

$$\frac{\partial \Delta}{\partial \dot{\delta}_i} = \frac{\partial F}{\partial \dot{\delta}_i} + \frac{\partial G}{\partial \dot{\delta}_i}.$$

4.2 First Order Bivariate Polynomial Case

Assume that

$$F(\delta_1, \dot{\delta}_1) = a_1 \delta_1 + a_2 \delta_1 v + a_0$$

and

$$G(\delta_2, \dot{\delta}_2) = b_1 \delta_2 + b_2 \dot{\delta}_2 v + b_0$$

then

$$\begin{aligned} \delta_1 &= K_z \delta \\ \dot{\delta}_1 &= K_z \dot{\delta} \end{aligned} \tag{54}$$

where

$$K_z = \frac{b_1 \delta + v b_2 \dot{\delta} + b_0 - a_0}{(a_1 + b_1) \delta + v(a_2 + b_2) \dot{\delta}},$$

$$v = \min\left(1, \frac{\delta}{\hat{\delta}}\right)$$

and

$\hat{\delta}$ is the inputted deflection at which the rate terms become fully effective.

4.3 Sixth Order Univariate Polynomial Case

Assume that

$$F(\delta_1, \delta_1') = a_0 + a_1 \delta_1 + a_2 \delta_1^2 + a_3 \delta_1^3 + a_4 \delta_1^4 + a_5 \delta_1^5 + a_6 \delta_1^6$$

and

$$G(\delta_2, \delta_2') = b_0 + b_1 \delta_2 + b_2 \delta_2^2 + b_3 \delta_2^3 + b_4 \delta_2^4 + b_5 \delta_2^5 + b_6 \delta_2^6$$

then δ_1 is the appropriate solution of

$$c_6 \delta_1^6 + c_5 \delta_1^5 + c_4 \delta_1^4 + c_3 \delta_1^3 + c_2 \delta_1^2 + c_1 \delta_1 + c_0 = 0 \quad (55)$$

where

$$c_0 = b_6 \delta^6 + b_5 \delta^5 + b_4 \delta^4 + b_3 \delta^3 + b_2 \delta^2 + b_1 \delta + b_0 - a_0$$

$$c_1 = 6 b_6 \delta^5 + 5 b_5 \delta^4 + 4 b_4 \delta^3 + 3 b_3 \delta^2 + 2 b_2 \delta + b_1 + a_1$$

$$c_2 = 15 b_6 \delta^4 + 10 b_5 \delta^3 + 6 b_4 \delta^2 + 3 b_3 \delta - b_2 + a_2$$

$$c_3 = 20 b_6 \delta^3 + 10 b_5 \delta^2 + 4 b_4 \delta + b_3 + a_3$$

$$c_4 = 15 b_6 \delta^2 + 5 b_5 \delta - b_4 + a_4$$

$$c_5 = 6 b_6 \delta + b_5 + a_5$$

$$c_6 = b_6 - a_6$$

4.4 General Pure Deflection Case

In this case,

$$F(\delta_1, \dot{\delta}_1) = f(\delta_1)$$

$$G(\delta_2, \dot{\delta}_2) = g(\delta_2)$$

where f and g are arbitrary functions of the appropriate deflections. Likewise Δ becomes a single variable function in terms of δ_1 and the task to find its appropriate zero. We use a three step iteration, the first of which takes advantage of the previous history.

$$\delta_1(t) = \delta_1(t - \Delta t) + \frac{G'(\delta - \delta_1)|_{t=t-\Delta t} [\delta(t) - \delta(t - \Delta t)]}{[F'(\delta_1) + G'(\delta - \delta_1)]|_{t=t-\Delta t}} \quad (56)$$

where

$$G'(\delta - \delta_1) = \frac{dG}{d\delta_1}$$

$$F'(\delta_1) = \frac{dF}{d\delta_1}$$

The second step is a direct application of Newton's method.

$$\delta_{12} = \delta_{11} - \frac{\Delta(\delta_{11})}{\Delta'(\delta_{11})} \quad (57)$$

where

the second subscript on the δ 's signifies the iteration step number and

$$\Delta' = \frac{d\Delta}{d\delta_1} = F' + G' \quad (58)$$

The third step employed depends upon the outcome of the second step. If the second step or any later step is on the opposite side of the zero of $\Delta(\delta_1)$ from the previous step, the method of halving the interval is employed to complete the iteration.

$$\delta_{1,m} = \frac{1}{2} (\delta_{1+} + \delta_{1-})$$

where δ_{1+} and δ_{1-} are chosen from all previous values of δ_1 such that $\Delta(\delta_{1+}) > 0$, $\Delta(\delta_{1-}) < 0$, and $|\delta_{1+} - \delta_{1-}|$ is minimized.

If at the third step or later steps it has not yet happened that two evaluations of $\Delta(\delta_1)$ have straddled the zero point, the classical secant method is employed.

$$\delta_{1,m} = \delta_{1,m-1} - \frac{\Delta(\delta_{1,m-1}) [\delta_{1,m-1} - \delta_{1,m-2}]}{\Delta(\delta_{1,m-2}) - \Delta(\delta_{1,m-1})}$$

This type of step is continued until a point is obtained for which the value of $\Delta(\delta_1)$ has the opposite sign of previous evaluations. The total number of steps due to all methods is limited to an inputted number.

4.5 Tabular Case

If the loading force of at least one of the materials is specified to be tabular, then the approach taken is to reduce the problem to a sequence of simple problems, each with a range of validity. When a solution is found within the range of validity, then the solution is accepted. If not, the problem is set up again shifting the range of validity in the direction of the last invalid solution.

A table is always reduced to a planar form: $F = a\delta_i + b\delta_i + c$ with the range of validity determined from the table points used to compute the coefficients.

If a polynomial is involved and the polynomial is linear, then the algorithm of Section 4.2 is used to obtain a tentative solution. If the polynomial is pure deflection, then the algorithm of Section 4.3 is tried. Any other case, the algorithm of Section 4.1 is used. Work remains to be done in the handling of table-general polynomial. The thought is to set up a planar form of limited validity for the general poly-

nomial as well as for the table and use Section 4.2. The details of the appropriate reduction of the general polynomial to planar form with the same range of validity as the planar form fitted to the table remains incomplete at this writing as does better handling of the pure deflection-bivariate table case.